Journal of Solid State Chemistry **168,** 408–417 (2002)
doi:10.1006/jssc.2002.9688

Crystal Structures, and Electrical Conducting and Magnetic Properties in the Plate Crystals of (Ethylenedithiotetrathiafulvalenoquinone-1, 3-dithiolemethide)$_2 \cdot MX_4$ (M=Fe, Ga, X=Br; M=Fe, X=Cl) Salts

Takuya Matsumoto,* Tsuyoshi Kominami,* Kazumasa Ueda,* Toyonari Sugimoto,*,†,[1] Toshiji Tada,* Harukazu Yoshino,‡ Keizo Murata,‡ Motoo Shiro,§ Ei-ichi Negishi,¶ Hiroshi Matsui,¶ Naoki Toyota,†,¶ Satoshi Endo,‖ and Kazuko Takahashi†

*Research Institute for Advanced Science and Technology, Osaka, Prefecture University, Osaka 599-8570, Japan; †Center for Interdisciplinary Research, Tohoku University, Sendai 980-8577, Japan; ‡Graduate School of Science, Osaka City University, Osaka 558-8585, Japan; §Rigaku Corporation, Tokyo 196-8666, Japan; ¶Graduate School of Science, Tohoku University, Sendai 980-8578, Japan; and ‖Center for Low-Temperature Science, Tohoku University, Sendai 980-8577, Japan

Received December 17, 2001; in revised form May 1, 2002; accepted May 13, 2002

By the reaction of a new donor molecule, ethylenedithiotetrathiafulvalenoquinone-1,3-dithiolemethide (1) with $FeBr_3$, $GaBr_3$ or $FeCl_3$ in CH_3CN/CS_2 charge transfer (CT) salts of 1 with counteranions of $FeBr_4^-$, $GaBr_4^-$ or $FeCl_4^-$ ($1_2 \cdot FeBr_4$, $1_2 \cdot GaBr_4$ and $1_2 \cdot FeCl_4$) as plate crystals were obtained. Their crystal structures are apparently similar to each other, in which 1 molecules are dimerized in the parallel direction of their molecular long axes, and the dimers are stacked with changing the direction of the molecular long axes alternately to form a one- dimensional column. The counteranions intervene between the 1-stacked columns and are aligned in a zigzag manner. The room-temperature electrical conductivities of $1_2 \cdot FeBr_4$ and $1_2 \cdot GaBr_4$ are fairly high (10–15 S cm^{-1}), but a small value (0.8 S cm^{-1}) is obtained for $1_2 \cdot FeCl_4$. For all CT salts, temperature dependences of electrical conductivity are semiconducting in spite of very small activation energies (30–90 meV). Based on the comparison between their electrical conducting and magnetic properties, it is suggested that the d spins of $FeBr_4^-$ or $FeCl_4^-$ ions exert almost no influence on the π conducting electrons in the 1-stacked column. © 2002 Elsevier Science (USA)

Key Words: **new donor molecule; charge-transfer salt; magnetic anion; high electrical conductivity; semiconducting; very small π–d interaction.**

INTRODUCTION

From about the middle of 1980 began an active study on molecular/organic magnetic conductors in which conducting electrons and local spins are expected to significantly interact with each other so as to produce novel electrical conducting and/or magnetic properties (1). Until now, there was a great deal of progress especially in several charge transfer (CT) salts of π donor molecules with magnetic-metal counteranions. In such molecular/organic π/d systems where the π electrons are conducting and the d spins are localized, the following are the most epoch making, that is, paramagnetic superconductors based on β''-[bis(ethylenedithio)tetrathiafulvalene (BEDT-TTF)$_4 \cdot$ [$(H_2O)M(C_2O_4)$]$_3 \cdot$ PhCN (M = Fe, Cr) (2, 3), antiferromagnetic superconductors based on κ-[bis(ethylenedithio) tetraselenafulvalene (BETS)]$_2 \cdot FeBr_4$ (4, 5), a ferromagnetic metal based on (BEDT-TTF)$_2 \cdot$[$MnCr(C_2O_4)_3$] (6), and a field-induced ferromagnetic superconductor based on λ-(BETS)$_2 \cdot FeCl_4$ (7). However, the simultaneous appearance of anitiferro- or ferromagnetism and metallic- or superconductivity is not always a result of the interaction between the conducting π electrons and the local d spins involved in the CT salts. The π/d interaction is scarcely present or very weak in the CT salts other than λ-(BETS)$_2 \cdot FeCl_4$ (8) and κ-(BETS)$_2 \cdot FeBr_4$ (4, 5), in which significant interaction however begins to occur at temperatures lower than 10 K. Because of these circumstances, current attention is directed toward developing new molecular/organic systems with much stronger π/d interaction. Very recently, we have succeeded in the synthesis of new donor molecules, tetrathiafulvaleno-thioquinone-1,3-dithiolemethides and -quinone-1,3-dithiolemethides substituted with two methylthio or one ethylenedithio groups (9, 10), which have an electron-donating ability comparable to TTF and can also capture several magnetic-metal salts via coordination to the thiocarbonyl sulfur or carbonyl oxygen atom. Indeed, the thioquinones formed 1:1 complexes with

[1] To whom correspondence should be addressed at Research Institute for Advanced Science and Technology, Osaka, Prefecture University, Osaka 599-8570, Japan. Fax: +81-72-252-4175; E-mail: toyonari@riast.osakafu-u.ac.jp.

0022-4596/02 $35.00

$CuBr_2$ (11). Especially for the complex of the ethylenedithio-substituted derivative comparatively high room-temperature electrical conductivity ($4\,S\,cm^{-1}$) was observed by virtue of moderate electron transfer from the thioquione to $CuBr_2$ moieties. However, as a result of semiconducting property with comparatively large activation energy of 0.18 eV, the *d* spins partly residing on the $CuBr_2$ moieties were subject to very weak and antiferromagnetic interaction. When $CuCl_2$, $FeCl_3$ or $FeBr_3$ were used in the place of $CuBr_2$ as a coordination partner for the thioquinones, instead of a complex such as the above CT salts with counteranions of $CuCl_4^{2-}$ (10), $FeCl_4^-$ (12) and $FeBr_4^-$ (12) were obtained, whose electrical conducting properties were semiconducting or insulating, as also expected from the fact that each of the thioquinones molecules forming a one-dimensional stacking are charged $+1$ or $+2/3$. Furthermore, it was probable that the *d* spins of the counteranions have no significant interaction with each other by aid of the conducting π electrons. The reaction of the quinones with $CuCl_2$, $CuBr_2$, $FeCl_3$ or $FeBr_3$ remain uninvestigated so far. First of all, we investigated the reaction of the ethylenedithio-substituted derivative (**1**) with $FeCl_3$ or $FeBr_3$, and also with the corresponding non-magnetic $GaBr_3$. In all the cases, the CT salts with counteranions of $FeCl_4^-$, $FeBr_4^-$ or $GaBr_4^-$ were obtained, which have a composition in the ratio of **1**:counteranion = 2:1, that is, $\mathbf{1}_2 \cdot FeCl_4$, $\mathbf{1}_2 \cdot FeBr_4$ and $\mathbf{1}_2 \cdot GaBr_4$. If a uniform or quasi-uniform stacking of **1** was formed in the CT salts, each of the molecules will be charged $+\frac{1}{2}$, so that it is much expected that both metallic conductivity and

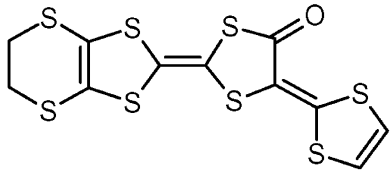

1

specific ordering of *d* spins of the magnetic counteranions are achieved. Here, we report on the crystal structures, and electrical conducting and magnetic properties of the three CT salts.

EXPERIMENTAL

Plate crystals of $\mathbf{1}_2 \cdot FeBr_4$, $\mathbf{1}_2 \cdot GaBr_4$ and $\mathbf{1}_2 \cdot FeCl_4$ CT salts were prepared using a two-phase contact method. Thus, a solution of **1** (3 mg, 7.3×10^{-3} mmol) in CS_2 (5 mL) was contacted with a solution of $FeBr_3$ (22 mg, 7.3×10^{-2} mmol), $GaBr_3$ (23 mg, 7.3×10^{-2} mmol) or $FeCl_3$ (11.8 mg, 7.3×10^{-2} mmol) in CH_3CN (4 mL) at room temperature, and the two-phase solution was kept at room temperature. After about 1 week, black-colored plate crystals of $\mathbf{1}_2 \cdot FeBr_4$, $\mathbf{1}_2 \cdot GaBr_4$ and $\mathbf{1}_2 \cdot FeCl_4$ appeared at the interface between the two solutions. Their elemental analyses gave satisfactory results. Calcd for $\mathbf{1}_2 \cdot FeBr_4$ ($C_{22}H_{12}S_{18}O_2FeBr_4$): C, 22.08; H, 1.01. Found: C, 22.15; H, 1.20. Calcd for $\mathbf{1}_2 \cdot GaBr_4$ ($C_{22}H_{12}S_{18}O_2GaBr_4$): C, 21.82; H, 1.00. Found: C, 21.82; H, 1.02. Calcd for $\mathbf{1}_2 \cdot FeCl_4$ ($C_{22}H_{12}S_{18}O_2FeCl_4$): C, 25.93; H, 1.09. Found: C, 26.10; H, 1.11.

X-ray diffraction data were collected at 113 K for the plate crystals of $\mathbf{1}_2 \cdot FeBr_4$, $\mathbf{1}_2 \cdot GaBr_4$ and $\mathbf{1}_2 \cdot FeCl_4$ on a Rigaku RAXIS-RAPID imaging plate diffractometer with graphite monochromated Mo$K\alpha$ radiation ($\lambda = 0.71069$ Å). Table 1 shows the crystallographic data for their crystals. The structures were solved by direct methods (SIR92 (13), SIR97 (14), and DIRDIF94 (15)), and refined on F_0^2 with full-matrix least-squares analysis. Calculated positions of the hydrogen atoms [d(C−H) = 0.95Å] were included in the final calculations. All the calculations were performed by using the teXsan crystallographic software package of the Molecular Structure Corporation (16). For $\mathbf{1}_2 \cdot FeBr_4$, the final cycle of least-squares refinement on F_0^2 for 8095 data and 406 parameters converged to $wR_2(F_0^2) = 0.116$ for all the data and to $R_1 = 0.053$ for 8090 data with $I \geq -10.00\sigma(I)$. For $\mathbf{1}_2 \cdot GaBr_4$, the final cycle of least-squares refinement on F_0^2 for 7581 data and 406 parameters converged on $wR_2(F_0^2) = 0.094$ for all the data and to $R_1 = 0.035$ for 7576 data with $I \geq -3.00\sigma(I)$. For $\mathbf{1}_2 \cdot FeCl_4$, the final cycle of least-squares refinement on F_0^2 for 7992 data and 406 parameters converged to $wR_2(F_0^2) = 0.140$ for all the data and to $R_1 = 0.061$ for 7987 data with $I \geq -10.00\sigma(I)$. Atomic coordinates and isotropic thermal parameters are given in Table 2, and selected interatomic distances and bond angles in Table 3.

Electrical conductivity measurement was performed on each of the plate crystals of $\mathbf{1}_2 \cdot FeBr_4$, $\mathbf{1}_2 \cdot GaBr_4$ and $\mathbf{1}_2 \cdot FeCl_4$ using a four-probe method in the temperature range from 60–100 to 300 K. The contact to the electrode was performed with gold paste. The magnetic susceptibility (χ_{obs}) of the microcrystals of $\mathbf{1}_2 \cdot FeBr_4$ and $\mathbf{1}_2 \cdot FeCl_4$ was measured between 5 and 300 K under an applied field of 1 kOe using a SQUID magnetometer (MPMS XL, Quantum Design). The paramagnetic susceptibility (χ_p) was obtained by subtracting the diamagnetic contribution calculated by Pascal method (17) from χ_{obs}.

RESULTS AND DISCUSSION

Crystal Structures of $\mathbf{1}_2 \cdot FeBr_4$, $\mathbf{1}_2 \cdot GaBr_4$ and $\mathbf{1}_2 \cdot FeCl_4$

For $\mathbf{1}_2 \cdot FeBr_4$ and $\mathbf{1}_2 \cdot GaBr_4$, both crystals involve two crystallographically independent **1** molecules, which have almost the same structures. Each molecular skeleton excepting for the terminal ethylene group has very high

TABLE 1
Crystallographic Data for the Plate Crystals of $\mathbf{1}_2 \cdot FeBr_4$, $\mathbf{1}_2 \cdot GaBr_4$ and $\mathbf{1}_2 \cdot FeCl_4$

	$\mathbf{1}_2 \cdot FeBr_4$	$\mathbf{1}_2 \cdot GaBr_4$	$\mathbf{1}_2 \cdot FeCl_4$
Formula	$(C_{11}H_6OS_8)_2 \cdot FeBr_4$	$(C_{11}H_6OS_8)_2 \cdot GaBr_4$	$(C_{11}H_6OS_8)_2 \cdot FeCl_4$
Mr	1196.88	1210.73	1018.95
Crystal size (mm^3)	$0.10 \times 0.10 \times 0.10$	$0.15 \times 0.02 \times 0.02$	$0.15 \times 0.15 \times 0.02$
Crystal habit	Black plate	Black plate	Black plate
Crystal system	Monoclinic	Monoclinic	Monoclinic
Space group	$P2_1/c$	$P2_1/c$	$P2_1/c$
a (Å)	6.5131(3)	6.5398(1)	6.5021(3)
b (Å)	39.760(2)	39.7885(8)	39.014(2)
c (Å)	13.944(1)	13.9312(3)	13.9108(7)
α (deg)	90.000	90.000	90.000
β (deg)	97.392(2)	97.416(1)	98.773(2)
γ (deg)	90.000	90.000	90.000
Cell volume ($Å^3$)	3580.8(4)	3594.7(1)	3487.5(3)
Z	4	4	4
Temperature (K)	113	113	113
ρ ($g\,cm^{-3}$)	2.116	2.237	1.941
$\mu_{MoK\alpha}$ (cm^{-1})	54.69	61.82	17.24
θ_{max}	54.8	55.0	55.0
Scan type	ω	ω	ω
Unique data	8090	7576	7986
R_{merge}	0.08	0.05	0.14
Weighting scheme	$1/\sigma^2\ (F_0^2)$	$1/\sigma^2\ (F_0^2)$	$1/\sigma^2\ (F_0^2)$
Residual electron density (min, max) ($e\,Å^3$)	−1.23, 1.25	−0.99, 0.76	−1.40, 1.34
Number of parameters refined	406	406	406
R_1	0.053	0.035	0.061
R_w	0.116	0.094	0.139

planarity, although the twisted angles between different rings are 1–6°.

The projections down to *bc* and *ab* planes for the crystal structure of $\mathbf{1}_2 \cdot FeBr_4$ are shown in Figs. 1a and 1b, respectively. As seen from Fig. 1a, each of the two **1** molecules (**A** and **B**) have the same direction of their molecular long axes. The interplanar distance is 3.41 Å, which is fairly shorter than "π-cloud thickness (3.50 Å)". (18). Moreover, Fig. 2a shows that there is a very effective overlap between the central tetrathiafulvalene parts of **A** and **B**, which possess large atomic orbital coefficients in the highest occupied molecular orbital of **1** molecule, so that this pair can be regarded as a dimer. Such **A**/B dimers are stacked along the *c*-axis with changing the direction of the molecular long axes alternately to form a one-dimensional column. In contrast to the **A**/B contact, the **B**/**A**′ overlap between the dimers is not effective (see Fig. 2b), although the interplanar distance (3.47 Å) is slightly shorter than "π-cloud thickness." On the other hand, there are also effective side-by-side contacts between **A**/**A**, **B**/**B** and **A**/**B**. The short contacts are seen between the S atom of an ethylenedithio group of one **A(B)** molecule and the S atoms of a 1,3-dithiole ring and an ethylenedithio group of the other **A(B)** molecule, and their distances are 3.52 (3.50) and 3.48 (3.58) Å, respectively, which are fairly shorter than the sum (3.70 Å) of van der Waals' radii of two S atoms (18). In addition, there is a short contact of S atoms (3.49 Å) between a 1,3-dithiolane-2thione ring of **A** and a 1,3-dithiole ring of **B**. The stacking structure of **1** molecules in $\mathbf{1}_2 \cdot GaBr_4$ is very similar to that in $\mathbf{1}_2 \cdot FeBr_4$, but there is a very small difference. It is a matter of course, since both $GaBr_4^-$ and $FeBr_4^-$ ions have almost the same tetrahedral-like geometry around the central Ga and Fe atoms, and have almost the same volume, except that $GaBr_4^-$ ion is non-magnetic in contrast to the magnetic $FeBr_4^-$ ion. The interplanar distances between **A**/**B** (**A**′/**B**′) and **B**/**A**′ are 3.40 and 3.48 Å, which are shorter and longer by 0.01 Å than the corresponding values in $\mathbf{1}_2 \cdot FeBr_4$, respectively. In addition, the side-by-side contacts between **A**/**A**, **B**/**B** and **A**/**B** have slightly different distances by 0.01 Å from those in $\mathbf{1}_2 \cdot FeBr_4$, except for the prolonged contact (3.70 Å) of S atoms between a 1,3-dithiolane-2-thione ring of **A** and a 1,3-dithiole ring of **B**.

On the other hand, the $FeBr_4^-$ ions in $\mathbf{1}_2 \cdot FeBr_4$ and the $GaBr_4^-$ ions in $\mathbf{1}_2 \cdot GaBr_4$ have both a slightly distorted tetrahedral geometry, since the six Br–Fe–Br bond angles (105.4°, 108.2°, 108.8°, 110.0°, 111.7° and 112.6°) for the $FeBr_4^-$ ion, and the six Br–Ga–Br bond angles (105.2°, 108.4°, 109.1°, 110.4°, 111.8° and 111.8°) for the $GaBr_4^-$ ion are significantly different from each other, although the

TABLE 2
Fractional Atomic Coordinates and Equivalent Isotropic Temperature Factors (Å)

Atom	x	y	z	U_{eq}
(1) *For* $\mathbf{1}_2 \cdot FeBr_4$				
Br(1)	1.0853(1)	0.02989(2)	0.90307(5)	0.0308(2)
Br(2)	1.0893(1)	0.09961(2)	0.72481(7)	0.0355(2)
Br(3)	0.5913(1)	0.04968(2)	0.73959(6)	0.0336(2)
Br(4)	1.0300(1)	0.00756(2)	0.63192(6)	0.0341(2)
Fe(1)	0.9500(2)	0.04614(3)	0.74669(7)	0.0216(3)
S(1)	0.8987(3)	0.34865(5)	0.4761(1)	0.0266(5)
S(2)	0.4613(3)	0.33283(5)	0.4200(1)	0.0268(5)
S(3)	0.9860(3)	0.22791(5)	0.4978(1)	0.0242(5)
S(4)	0.5559(3)	0.25282(5)	0.4492(1)	0.0221(5)
S(5)	0.8461(3)	0.15338(5)	0.4642(1)	0.0222(5)
S(6)	0.4095(3)	0.17318(5)	0.4149(1)	0.0220(5)
S(7)	0.7703(3)	0.08065(5)	0.4651(2)	0.0303(5)
S(8)	0.2516(3)	0.10283(5)	0.4020(1)	0.0263(5)
S(9)	0.8210(3)	0.32350(5)	0.2184(1)	0.0231(5)
S(10)	0.4000(3)	0.29978(5)	0.1634(1)	0.0227(5)
S(11)	0.9606(3)	0.20200(5)	0.2451(1)	0.0232(5)
S(12)	0.5280(3)	0.22440(4)	0.1960(1)	0.0216(5)
S(13)	0.8085(3)	0.12539(4)	0.2149(1)	0.0218(5)
S(14)	0.3819(3)	0.14847(5)	0.1649(1)	0.0227(5)
S(15)	0.7181(3)	0.05342(5)	0.1806(2)	0.0327(6)
S(16)	0.2043(3)	0.08223(5)	0.1189(1)	0.0294(5)
O(1)	1.1084(8)	0.2908(1)	0.5144(4)	0.031(2)
O(2)	1.0670(8)	0.2661(1)	0.2705(3)	0.027(1)
C(1)	0.732(1)	0.3821(2)	0.4436(5)	0.030(2)
C(2)	0.534(1)	0.3749(2)	0.4163(5)	0.031(2)
C(3)	0.708(1)	0.3177(2)	0.4571(5)	0.022(1)
C(4)	0.957(1)	0.2726(2)	0.4954(5)	0.022(1)
C(5)	0.750(1)	0.2836(2)	0.4705(5)	0.022(2)
C(6)	0.726(1)	0.2183(2)	0.4623(5)	0.021(1)
C(7)	0.664(1)	0.1861(2)	0.4483(5)	0.021(1)
C(8)	0.662(1)	0.1207(2)	0.4447(5)	0.022(2)
C(9)	0.465(1)	0.1299(2)	0.4221(5)	0.020(1)
C(10)	0.546(1)	0.0530(2)	0.4467(6)	0.029(2)
C(11)	0.350(1)	0.0680(2)	0.4763(6)	0.030(2)
C(12)	0.632(1)	0.3535(2)	0.1809(5)	0.022(2)
C(13)	0.442(1)	0.3424(2)	0.1542(5)	0.024(2)
C(14)	0.652(1)	0.2895(2)	0.2013(5)	0.018(1)
C(15)	0.713(1)	0.2564(2)	0.2168(5)	0.020(2)
C(16)	0.924(1)	0.2471(2)	0.2467(5)	0.022(1)
C(17)	0.703(1)	0.1917(2)	0.2121(5)	0.020(1)
C(18)	0.637(1)	0.1586(2)	0.1989(5)	0.021(1)
C(19)	0.620(1)	0.0947(2)	0.1793(5)	0.024(2)
C(20)	0.426(1)	0.1055(2)	0.1569(5)	0.024(1)
C(21)	0.497(1)	0.0321(2)	0.1177(6)	0.031(2)
C(22)	0.296(1)	0.0409(2)	0.1526(5)	0.028(2)
(2) *For* $\mathbf{1}_2 \cdot GaBr_4$				
Br(1)	−0.08570(7)	0.47041(1)	0.09771(3)	0.0286(1)
Br(2)	0.40775(6)	0.45000(1)	0.25904(3)	0.0306(1)
Br(3)	−0.08943(6)	0.40066(1)	0.27374(4)	0.0299(1)
Br(4)	−0.02699(7)	0.49135(1)	0.36942(3)	0.0306(1)
Ga(1)	0.05162(7)	0.45364(1)	0.25291(3)	0.0201(1)
S(1)	0.7504(2)	0.39655(3)	0.59602(8)	0.0247(3)
S(2)	0.2311(2)	0.41912(3)	0.53253(9)	0.0270(3)
S(3)	0.5912(1)	0.32642(3)	0.58345(7)	0.0199(2)
S(4)	0.1552(1)	0.34638(3)	0.53379(7)	0.0205(2)
S(5)	0.4437(1)	0.24687(2)	0.54817(7)	0.0198(2)
S(6)	0.0149(1)	0.27197(3)	0.50016(8)	0.0223(2)
S(7)	0.5374(2)	0.16694(3)	0.57775(8)	0.244(3)
S(8)	0.1012(2)	0.15124(3)	0.52214(8)	0.0246(3)
S(9)	0.6010(1)	0.20039(3)	0.83466(8)	0.0221(3)
S(10)	0.1810(2)	0.17650(3)	0.77944(7)	0.0214(2)
S(11)	0.4726(1)	0.27557(2)	0.80149(8)	0.0205(2)
S(12)	0.0408(1)	0.29804(3)	0.75272(8)	0.0216(2)
S(13)	0.6194(2)	0.35140(3)	0.83288(8)	0.0215(2)
S(14)	0.1930(1)	0.37457(3)	0.78363(7)	0.0207(2)
S(15)	0.7975(2)	0.41748(3)	0.87944(9)	0.0276(3)
S(16)	0.2840(2)	0.44644(3)	0.81874(9)	0.302(3)
O(1)	−0.1093(4)	0.20890(7)	0.4835(2)	0.0278(8)
O(2)	−0.0644(4)	0.23390(7)	0.7278(2)	0.0283(8)
C(1)	0.6495(6)	0.4320(1)	0.5218(3)	0.028(1)
C(2)	0.4544(7)	0.4463(1)	0.5534(3)	0.027(1)
C(3)	0.5361(6)	0.36992(10)	0.5767(3)	0.0205(10)
C(4)	0.3380(6)	0.3791(1)	0.5518(3)	0.0209(10)
C(5)	0.3355(6)	0.31379(10)	0.5496(3)	0.0177(9)
C(6)	0.2747(6)	0.28114(10)	0.5353(3)	0.0184(9)
C(7)	0.2514(6)	0.21608(10)	0.5290(3)	0.0191(10)
C(8)	0.0416(6)	0.2272(1)	0.5018(3)	0.023(1)
C(9)	0.2918(6)	0.18216(10)	0.5403(3)	0.0188(10)
C(10)	0.4648(7)	0.1249(1)	0.5810(3)	0.030(1)
C(11)	0.2673(7)	0.1179(1)	0.5548(3)	0.029(1)
C(12)	0.5600(7)	0.1577(1)	0.8440(3)	0.025(1)
C(13)	0.3689(7)	0.14698(10)	0.8174(3)	0.025(1)
C(14)	0.3483(6)	0.21036(10)	0.7958(3)	0.0177(9)
C(15)	0.2896(6)	0.24370(10)	0.7817(3)	0.0185(9)
C(16)	0.0794(6)	0.2531(1)	0.7507(3)	0.022(1)
C(17)	0.2991(6)	0.3085(1)	0.7860(3)	0.0205(10)
C(18)	0.3627(6)	0.34098(10)	0.7984(3)	0.0185(10)
C(19)	0.5753(6)	0.3944(1)	0.8411(3)	0.023(1)
C(20)	0.3785(6)	0.4053(1)	0.8188(3)	0.0215(10)
C(21)	0.7070(7)	0.4592(1)	0.8476(3)	0.026(1)
C(22)	0.5056(7)	0.4677(1)	0.8831(3)	0.026(1)
(3) *For* $\mathbf{1}_2 \cdot FeCl_4$				
Fe(1)	0.9637(2)	0.45377(3)	0.23862(9)	0.0289(3)
Cl(1)	1.1062(3)	0.46788(5)	0.3875(2)	0.0393(6)
Cl(2)	1.0301(4)	0.49162(5)	0.1316(2)	0.0426(7)
Cl(3)	0.6262(3)	0.45053(6)	0.2342(2)	0.0386(6)
Cl(4)	1.0928(3)	0.40284(5)	0.2133(2)	0.0436(7)
S(1)	0.7692(3)	0.42205(5)	−0.0373(2)	0.0328(6)
S(2)	0.2439(3)	0.40005(5)	−0.0991(2)	0.0307(6)
S(3)	0.8420(3)	0.34770(5)	−0.0375(2)	0.0265(6)
S(4)	0.3991(3)	0.32810(5)	−0.0873(2)	0.0255(6)
S(5)	0.9785(3)	0.27124(5)	−0.0056(2)	0.0289(6)
S(6)	0.5425(3)	0.24665(5)	−0.0561(2)	0.0260(6)
S(7)	0.8789(3)	0.14818(5)	−0.0270(2)	0.0306(6)
S(8)	0.4394(3)	0.16514(5)	−0.0847(2)	0.0310(6)
S(9)	0.6969(3)	0.45055(5)	−0.3187(2)	0.364(6)
S(10)	0.1793(3)	0.42078(5)	−0.3849(2)	0.333(6)
S(11)	0.7919(3)	0.37721(5)	−0.2872(2)	0.0274(6)
S(12)	0.3627(3)	0.35333(5)	−0.3392(2)	0.0267(6)
S(13)	0.9528(3)	0.29997(5)	−0.2577(2)	0.0282(6)
S(14)	0.5193(3)	0.27548(5)	−0.3081(2)	0.0269(6)
S(15)	0.8307(3)	0.17580(5)	−0.2829(2)	0.0300(6)
S(16)	0.4001(3)	0.19794(5)	−0.3378(2)	0.0290(6)
O(1)	1.0962(8)	0.2063(1)	0.0114(4)	0.034(2)
O(2)	0.0690(8)	0.2349(1)	−0.2337(4)	0.033(2)
C(1)	0.546(1)	0.4504(2)	−0.0538(6)	0.037(3)

TABLE 2—*Continued*

Atom	*x*	*y*	*z*	U_{eq}
C(2)	0.352(1)	0.4353(2)	−0.0223(6)	0.032(2)
C(3)	0.662(1)	0.3814(2)	−0.0549(6)	0.024(2)
C(4)	0.456(1)	0.3724(2)	−0.0794(6)	0.022(2)
C(5)	0.657(1)	0.3146(2)	−0.0549(6)	0.021(2)
C(6)	0.715(1)	0.2817(2)	−0.0413(6)	0.028(2)
C(7)	0.947(1)	0.2256(2)	−0.0087(6)	0.031(2)
C(8)	0.734(1)	0.2148(2)	−0.0364(6)	0.025(2)
C(9)	0.689(1)	0.1801(2)	−0.0459(6)	0.026(2)
C(10)	0.707(1)	0.1145(2)	−0.0605(6)	0.033(3)
C(11)	0.505(1)	0.1221(2)	−0.0861(7)	0.035(3)
C(12)	0.472(1)	0.4718(2)	−0.3850(7)	0.035(3)
C(13)	0.269(1)	0.4631(2)	−0.3520(6)	0.035(3)
C(14)	0.603(1)	0.4081(2)	−0.3218(6)	0.027(2)
C(15)	0.405(1)	0.3974(2)	−0.3450(6)	0.027(2)
C(16)	0.623(1)	0.3427(2)	−0.3044(6)	0.027(2)
C(17)	0.691(1)	0.3097(2)	−0.2907(6)	0.022(2)
C(18)	0.918(1)	0.2541(2)	−0.2581(6)	0.028(2)
C(19)	0.708(1)	0.2433(2)	−0.2871(6)	0.026(2)
C(20)	0.654(1)	0.2092(2)	−0.3002(6)	0.027(2)
C(21)	0.644(1)	0.1442(2)	−0.3192(6)	0.34(3)
C(22)	0.449(1)	0.1545(2)	−0.3455(6)	0.034(3)

TABLE 3
Selected Interatomic Distance for (Å) and Angles (deg)

(1) *For* $\mathbf{1}_2 \cdot FeBr_4$

Br(1)–Fe(1)	2.336(1)	S(12)–C(15)	1.751(8)
Br(2)–Fe(1)	2.347(1)	S(12)–C(17)	1.725(8)
Br(3)–Fe(1)	2.330(2)	S(13)–C(18)	1.725(8)
Br(4)–Fe(1)	2.324(1)	S(13)–C(19)	1.757(7)
S(1)–C(1)	1.740(8)	S(14)–C(18)	1.716(7)
S(1)–C(3)	1.744(8)	S(14)–C(20)	1.738(8)
S(2)–C(2)	1.741(8)	S(15)–C(19)	1.761(8)
S(2)–C(3)	1.731(7)	S(15)–C(21)	1.799(7)
S(3)–C(4)	1.787(8)	S(16)–C(20)	1.739(7)
S(3)–C(6)	1.744(7)	S(16)–C(22)	1.790(8)
S(4)–C(5)	1.757(7)	O(1)–C(4)	1.224(8)
S(4)–C(6)	1.759(8)	O(2)–C(16)	1.212(8)
S(5)–C(7)	1.755(8)	C(1)–C(2)	1.328(9)
S(5)–C(8)	1.765(8)	C(3)–C(5)	1.39(1)
S(6)–C(7)	1.741(7)	C(4)–C(5)	1.417(9)
S(6)–C(9)	1.759(8)	C(6)–C(7)	1.35(1)
S(7)–C(8)	1.750(8)	C(8)–C(9)	1.332(9)
S(7)–C(10)	1.820(7)	C(10)–C(11)	1.51(1)
S(8)–C(9)	1.752(2)	C(12)–C(13)	1.321(9)
S(8)–C(11)	1.798(8)	C(14)–C(15)	1.38(1)
S(9)–C(12)	1.745(7)	C(15)–C(16)	1.432(9)
S(9)–C(14)	1.740(8)	C(17)–C(18)	1.39(1)
S(10)–C(13)	1.724(8)	C(19)–C(20)	1.33(9)
S(10)–C(14)	1.708(7)	C(21)–C(22)	1.50(1)
S(11)–C(16)	1.810(8)		
S(11)–C(17)	1.731(7)		

Br(1)–Fe(1)–Br(2)	105.44(5)	Br(2)–Fe(1)–Br(3)	110.00(6)
Br(1)–Fe(1)–Br(3)	108.19(5)	Br(2)–Fe(1)–Br(4)	112.57(6)
Br(1)–Fe(1)–Br(4)	111.67(6)	Br(3)–Fe(1)–Br(4)	108.85(5)

TABLE 3—*Continued*

(2) *For* $\mathbf{1}_2 \cdot GaBr_4$

Br(1)–Ga(1)	2.3292(6)	S(12)–C(16)	1.807(4)
Br(2)–Ga(1)	2.3241(6)	S(12)–C(17)	1.743(4)
Br(3)–Ga(1)	3.3341(6)	S(13)–C(18)	1.736(4)
Br(4)–Ga(1)	2.3164(6)	S(13)–C(19)	1.741(4)
S(1)–C(1)	1.822(4)	S(14)–C(18)	1.732(4)
S(1)–C(3)	1.750(4)	S(14)–C(20)	1.747(4)
S(2)–C(2)	1.810(5)	S(15)–C(19)	1.744(4)
S(2)–C(4)	1.746(4)	S(15)–C(21)	1.799(4)
S(3)–C(3)	1.768(4)	S(16)–C(20)	1.750(4)
S(3)–C(5)	1.752(4)	S(16)–C(22)	1.812(4)
S(4)–C(4)	1.763(4)	O(1)–C(8)	1.226(5)
S(4)–C(5)	1.747(4)	O(2)–C(16)	1.222(5)
S(5)–C(6)	1.750(4)	C(1)–C(2)	1.513(6)
S(5)–C(7)	1.751(4)	C(3)–C(4)	1.348(5)
S(6)–C(6)	1.745(4)	C(5)–C(6)	1.366(6)
S(6)–C(8)	1.790(4)	C(7)–C(8)	1.445(5)
S(7)–C(9)	1.733(4)	C(7)–C(9)	1.380(6)
S(7)–C(10)	1.741(4)	C(10)–C(11)	1.326(6)
S(8)–C(9)	1.746(4)	C(12)–C(13)	1.327(6)
S(8)–C(11)	1.738(4)	C(14)–C(15)	1.388(6)
S(9)–C(12)	1.727(4)	C(15)–C(16)	1.436(5)
S(9)–C(14)	1.718(4)	C(17)–C(18)	1.362(6)
S(10)–C(13)	1.733(4)	C(19)–C(20)	1.356(5)
S(10)–C(14)	1.732(4)	C(21)–C(22)	1.504(7)
S(11)–C(16)	1.741(4)		
S(11)–C(17)	1.728(4)		

Br(1)–Ga(1)–Br(2)	108.45(3)	Br(2)–Ga(1)–Br(3)	110.45(2)
Br(1)–Ga(1)–Br(3)	105.24(2)	Br(2)–Ga(1)–Br(4)	109.06(2)
Br(1)–Ga(1)–Br(4)	111.78(2)	Br(3)–Ga(1)–Br(4)	111.77(3)

(3) *For* $\mathbf{1}_2 \cdot FeCl_4$

Fe(1)–Cl(1)	2.205(2)	S(12)–C(15)	1.744(8)
Fe(1)–Cl(2)	2.186(3)	S(12)–C(16)	1.739(7)
Fe(1)–Cl(3)	2.190(2)	S(13)–C(17)	1.737(7)
Fe(1)–Cl(4)	2.206(2)	S(13)–C(18)	1.805(8)
S(1)–C(1)	1.814(8)	S(14)–C(17)	1.732(7)
S(1)–C(3)	1.736(8)	S(14)–C(19)	1.747(8)
S(2)–C(2)	1.814(8)	S(15)–C(20)	1.728(8)
S(2)–C(4)	1.741(7)	S(15)–C(21)	1.750(8)
S(3)–C(3)	1.754(7)	S(16)–C(20)	1.711(8)
S(3)–C(5)	1.754(7)	S(16)–C(22)	1.730(8)
S(4)–C(4)	1.768(7)	O(1)–C(7)	1.223(9)
S(4)–C(5)	1.752(7)	O(2)–C(18)	1.240(8)
S(5)–C(6)	1.755(8)	C(1)–C(2)	1.52(1)
S(5)–C(7)	1.793(9)	C(3)–C(4)	1.371(10)
S(6)–C(6)	1.761(8)	C(5)–C(6)	1.344(19)
S(6)–C(8)	1.748(8)	C(7)–C(8)	1.44(1)
S(7)–C(9)	1.743(8)	C(8)–C(9)	1.389(10)
S(7)–C(10)	1.743(8)	C(10)–C(11)	1.34(1)
S(8)–C(9)	1.733(8)	C(12)–C(13)	1.50(1)
S(8)–C(11)	1.733(8)	C(14)–C(15)	1.35(1)
S(9)–C(12)	1.804(8)	C(16)–C(17)	1.366(10)
S(9)–C(14)	1.762(8)	C(18)–C(19)	1.429(10)
S(10)–C(13)	1.786(8)	C(19)–C(20)	1.38(1)
S(10)–C(15)	1.747(8)	C(21)–C(22)	1.33(1)
S(11)–C(14)	1.733(8)		
S(11)–C(16)	1.729(7)		

Cl(1)–Fe(1)–Cl(2)	111.87(9)	Cl(2)–Fe(1)–Cl(3)	108.71(10)
Cl(1)–Fe(1)–Cl(3)	108.46(10)	Cl(2)–Fe(1)–Cl(4)	112.3(1)
Cl(1)–Fe(1)–Cl(4)	105.03(10)	Cl(3)–Fe(1)–Cl(4)	110.33(9)

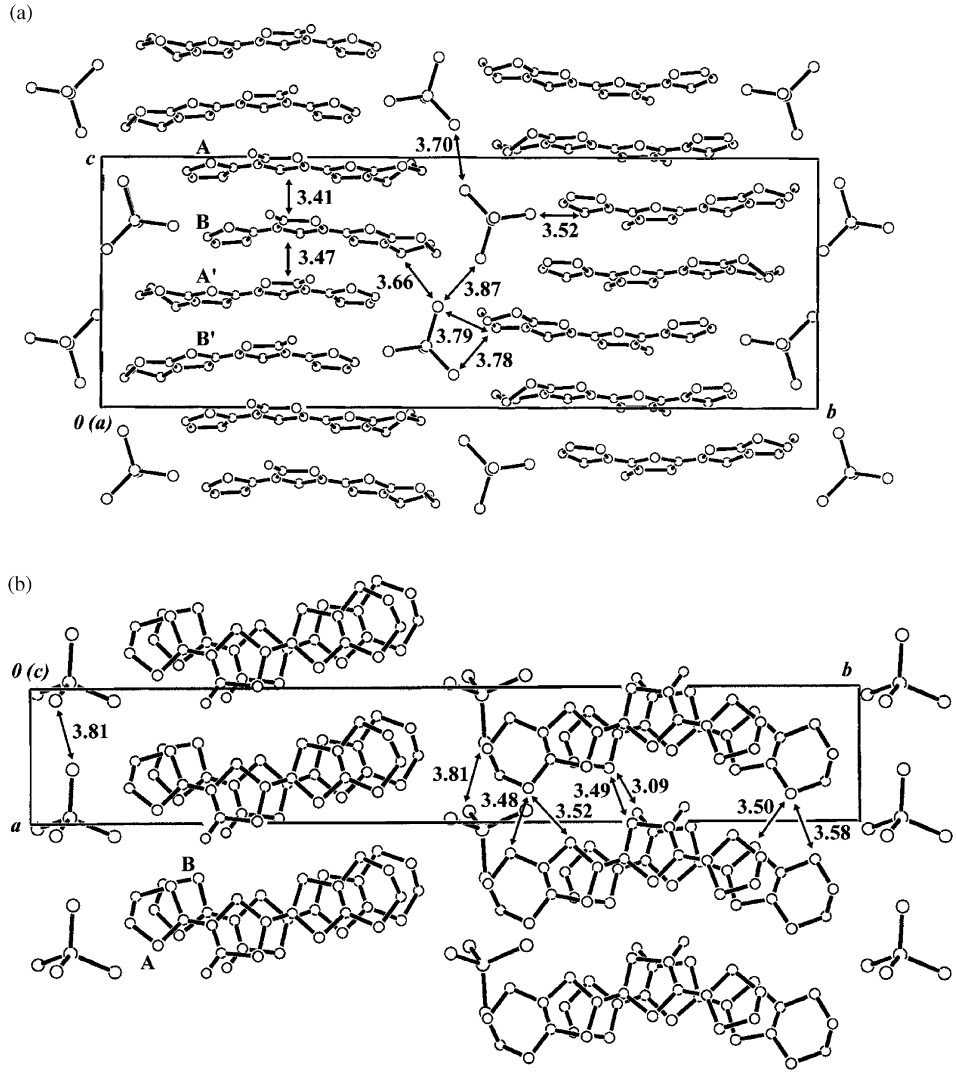

FIG. 1. The packing structure of the plate crystal of $\mathbf{1}_2 \cdot FeBr_4$: the projections down to (a) *bc* and (b) *ab* planes.

four Fe–Br and Ga–Br bond distances are almost the same (2.32–2.35 and 2.32–2.33 Å). Each $FeBr_4^-$ and $GaBr_4^-$ ions intervene between the **1**-stacked columns and are aligned along the *c*-axis with changing the direction of the geometry by 180° alternately in a zigzag manner. Such $FeBr_4^-$ and $GaBr_4^-$ ion arrays have alternation of two different Br–Br contacts with the distances of 3.70 and 3.87 Å for the $FeBr_4^-$ ion case, and of 3.67 and 3.87 Å for the $GaBr_4^-$ ion case which are both shorter than the sum (3.90 Å) of van der Waals' radii of the two Br atoms (18). The comparatively short Br–Br contacts with the distance of 3.81 Å for both the $FeBr_4^-$ and $GaBr_4^-$ ion cases are also seen between the neighboring arrays. In addition, there are several short contacts between the **1**-stacked column and the $FeBr_4^-$ or $GaBr_4^-$ ion, as seen between the S atoms of ethylenedithio or 1,3-dithiole groups and the Br atoms of $FeBr_4^-$ or $GaBr_4^-$ ion with shorter distances of 3.66, 3.78, 3.79 and 3.52 Å for the $FeBr_4^-$ ion case, and 3.70, 3.79, 3.83, and 3.54 Å for the $GaBr_4^-$ ion case than the sum (3.80 Å) of van der Waals' radii of S and Br atoms (see Fig. 1a) (18).

The crystal structure of $\mathbf{1}_2 \cdot FeCl_4$ is apparently similar to that of $\mathbf{1}_2 \cdot FeCl_4$, as can be seen from the projections down to *bc* and *ab* planes in Figs. 3a and 3b. However, the significant difference can be seen on the stacking of **1** molecules as well as on the contact between the neighboring counteranions. Thus, the interplanar distances in the intra- and inter-dimers in $\mathbf{1}_2 \cdot FeCl_4$ are 3.45 and 3.89 Å, respectively, which are much different from the corresponding values (3.41 and 3.47 Å) in $\mathbf{1}_2 \cdot FeBr_4$, although the overlapping modes between the **1** molecules in the intra- and inter-dimers are very similar to each other between the $FeCl_4^-$ and $FeBr_4^-$ salts. From the much

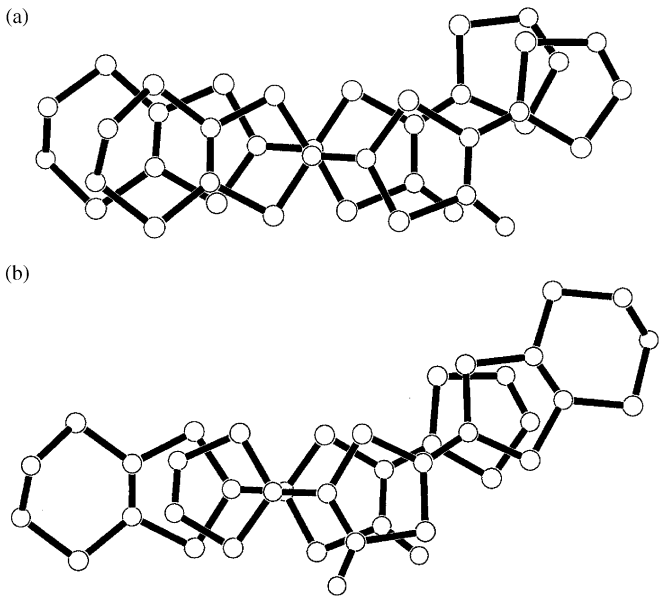

FIG. 2. The contacts of two neighboring **1** molecules (**A** and **B**) in the plate crystal of $\mathbf{1}_2 \cdot FeBr_4$: (a) **A/B** and (b) **B/A′** contacts.

increased difference in the distances between the intra- and inter-dimers in $\mathbf{1}_2 \cdot FeCl_4$ compared with that in $\mathbf{1}_2 \cdot FeBr_4$, the **1** molecules are much more preferentially dimerized in the stacking of $\mathbf{1}_2 \cdot FeCl_4$ than of $\mathbf{1}_2 \cdot FeBr_4$. Accompanied by the changed stacking of **1** molecules in $\mathbf{1}_2 \cdot FeCl_4$, the $FeCl_4^-$ ions also adopt a different location in the crystal space from the $FeBr_4^-$ ions in $\mathbf{1}_2 \cdot FeBr_4$. In addition, since the Fe–Cl bond distance (2.20 Å) is shorter than that (2.33 Å) of the Fe–Br bond, the shortest Cl–Cl contacts between the neighboring $FeCl_4^-$ ions have fairly different distances from the corresponding Br–Br contacts. Thus, one Cl–Cl contact in a zigzag chain of $FeCl_4^-$ ions along the stacking direction has a very close distance (3.68 Å) to the sum (3.67 Å) of van der Waals' radii of two Cl atoms (18). While, in the other Cl–Cl contact the distance (4.39 Å) is fairly long compared with the corresponding van der Waals' radii contact distance. There is also a long Cl–Cl contact (the distance: 3.91 Å) between the neighboring $FeCl_4^-$ ions in the direction perpendicular to the stacking.

Electrical Conductivities

Since all the plate crystals of $\mathbf{1}_2 \cdot FeBr_4$, $\mathbf{1}_2 \cdot GaBr_4$ and $\mathbf{1}_2 \cdot FeCl_4$ were very thin, four Au probes were only put on the wide plane for their electrical conductivity (σ) measurement. The σ values on the wide plane at room temperature were considerably high for $\mathbf{1}_2 \cdot FeBr_4$ ($15.5\,S\,cm^{-1}$) and $\mathbf{1}_2 \cdot GaBr_4$ ($10.5\,S\,cm^{-1}$), while not so high for $\mathbf{1}_2 \cdot FeCl_4$ ($0.8\,S\,cm^{-1}$). To determine the relationship between the crystal structure and the crystal shape analysis using a four-circle X-ray diffractometer with graphite-monochromated Mo$K\alpha$ radiation was attempted. It was however unsuccessful because any plate crystal was too thin to get intense diffractions from the thin plane. Accordingly, for the present it is unknown that the wide plane measured is parallel or perpendicular to the stacking of **1** molecules. Nevertheless, it is most probable that it is the stacking plane in view of the facts that the σ values are considerably high for $\mathbf{1}_2 \cdot FeBr_4$ and $\mathbf{1}_2 \cdot GaBr_4$ with the comparatively uniform **1**-stacked structure, while low for $\mathbf{1}_2 \cdot FeCl_4$ with the preferentially **1**-dimerized stacked structure. However, such a large difference in σ cannot be expected from the perpendicular plane to the stacking of **1** molecules, since the three crystals have almost the same interstacking structures. The temperature dependence of electrical resistivity (ρ, a reciprocal of σ) was investigated for the three crystals. As is obvious from the results shown in Fig. 4, in all the cases the ρ values continuously increased, as the temperature was gradually cooled down from 300 to 60–100 K, where a crack in the crystal suddenly occurred. The $\rho - T$ behavior in the temperature rage is due to a typical semiconductor. The activation energies are however very small for $\mathbf{1}_2 \cdot FeBr_4$ (57 meV) and $\mathbf{1}_2 \cdot GaBr_4$ (27 meV). In contrast, $\mathbf{1}_2 \cdot FeCl_4$ has a large value of 120 meV, as supposed from the fairly low room-temperature σ value compared with those of the $FeBr_4^-$ and $GaBr_4^-$ salts. In addition, it should be noted that significant change cannot be recognized in the electrical conducting properties in the temperature range of 300–60 K between $\mathbf{1}_2 \cdot FeBr_4$ and $\mathbf{1}_2 \cdot GaBr_4$, suggesting that the *d* spins of $FeBr_4^-$ ions exert no influence on the π conducting electrons in the **1**-stacked column in this temperature range. As mentioned next, the magnetic result on the temperature dependence of χ_p in $\mathbf{1}_2 \cdot FeBr_4$ showed that the *d* spins of $FeBr_4^-$ ions interact with each other, but there is no interaction between the *d* spins and the conducting π electrons in the temperature range of 300–60 K and also of 60–5 K.

Magnetic Properties

The temperature dependences of the product of χ_p with temperature ($\chi_p \cdot T$) for $\mathbf{1}_2 \cdot FeBr_4$ and $\mathbf{1}_2 \cdot FeCl_4$ in the temperature range of 5–300 K are shown in Fig. 5. The $\chi_p \cdot T$ values gradually decreased as the temperature was cooled down from 300 K, and such a trend continued till 5 K. This $\chi_p \cdot T - T$ behavior obviously shows preferential occurrence of antiferromagnetic interaction in the overall temperature range measured. The χ_p obtained can well be interpreted as the sum of a component obeying the Curie–Weiss law $C/(T - \theta)$, where C is the Curie constant and θ the Weiss temperature) and of an almost temperature-independent component (χ_π) in the low-temperature region of the $\chi_p - T$ curve obtained by strong antiferro-

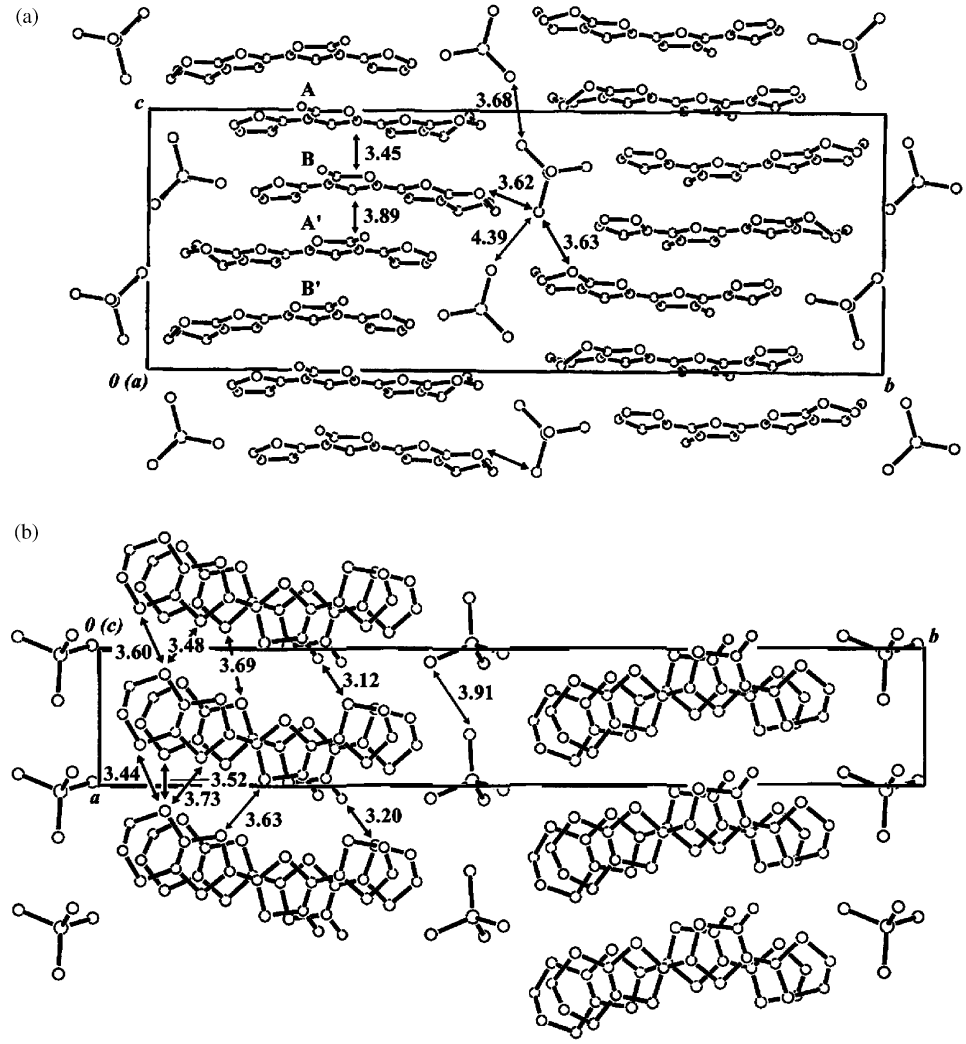

FIG. 3. The packing structure of the plate crystal of $\mathbf{1}_2 \cdot FeCl_4$: the projections down to (a) *bc* and (b) *ab* planes.

magnetically interacting spins in the semiconducting case. It is of course that the former component is due to the *d* spins of $FeBr_4^-$ or $FeCl_4^-$ ions and the latter component is related to the π conducting electrons in the **1**-stacked column. The best fitting between experimental and theoretical data gave $C = 4.59\,\text{emu K mol}^{-1}$, $\theta = -5.0\,\text{K}$ and $\chi_\pi = 5.5 \times 10^{-4}\,\text{emu mol}^{-1}$ for $\mathbf{1}_2 \cdot FeBr_4$, and $C = 4.57\,\text{emu K mol}^{-1}$, $\theta = -3.2\,\text{K}$ and $\chi_\pi = 3.6 \times 10^{-3}\,\text{emu mol}^{-1}$ for $\mathbf{1}_2 \cdot FeCl_4$. The *C* obtained is almost the same as the value ($4.60\,\text{emu K mol}^{-1}$) calculated as an Fe(III) spin entity with $S = 5/2$ and $g = 2.050$. The small value and negative sign in θ indicates very weak antiferromagnetic interaction between the Fe(III) *d* spins. The χ_π is close to the values observed in several organic semiconductors reported so far (10, 19–21). The different magnitude of interaction between the *d* spins of the $FeBr_4^-$ and $FeCl_4^-$ ions can be readily understood based on the different alignment of the $FeBr_4^-$ and $FeCl_4^-$ ions in a zigzag array. Thus, the Br–Br contacts in the $FeBr_4^-$ ion array have two slightly different distances of 3.70 and 3.87 Å, which are both shorter than the sum (3.90 Å) of van der Waals' radii of two Br atoms. But, for the Cl–Cl contacts in the $FeCl_4^-$ ion array the corresponding distances are 3.68 and 4.39 Å. The shorter one is comparable to the sum (3.67 Å) of van der Waals' radii of two Cl atoms, but the other one is too longer than the sum. Since the spins are effectively delocalized on the whole of $FeBr_4^-$ and $FeCl_4^-$ ions, some amount of the spins can also reside on each of the four Br and Cl atoms. Considering this spin distribution in the $FeBr_4^-$ and $FeCl_4^-$ ions together with their different alignment as mentioned above, the *d* spin interaction in the $FeCl_4^-$ ion array will be smaller than that in the $FeBr_4^-$ ion array. It is actually the case, as is obvious from the θ values observed. To detect the π conducting electrons

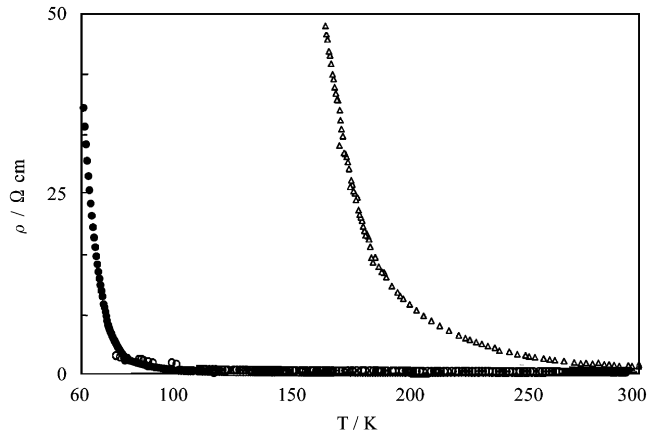

FIG. 4. The temperature dependence of electrical resistivity (ρ) for the plate crystal of (●)$\mathbf{1}_2 \cdot FeBr_4$, (○)$\mathbf{1}_2 \cdot GABr_4$ and (△) $\mathbf{1}_2 \cdot FeCl_4$.

involved in $\mathbf{1}_2 \cdot FeBr_4$ and $\mathbf{1}_2 \cdot FeCl_4$ their ESR measurements were performed. The ESR spectrum of the microcrystals of $\mathbf{1}_2 \cdot FeBr_4$ at room temperature showed one very weak signal ($g = 2.0062$ and $\Delta H_{pp} = 87$ Oe) due to the π conducting electrons in the **1**-stacked column together with one intensively strong and broad signal ($g = 2.0437$ and $\Delta H_{pp} = 1130$ Oe) due to the π conducting electrons in the **1**-stacked column together with one intensively strong and broad signal ($g = 2.0437$ and $\Delta H_{pp} = 1130$ Oe) (12) due to the d spins of $FeBr_4^-$ ions. The g and ΔH_{pp} values of the π signal are close to those ($g = 2.0062$ and $\Delta H_{pp} = 115$ Oe) obtained in $\mathbf{1}_2 \cdot GaBr_4$ without any d spins. The intensity of π signals in $\mathbf{1}_2 \cdot FeBr_4$ and $\mathbf{1}_2 \cdot GaBr_4$ was almost not changed in the measurement at 77 K. The ESR spectrum of the microcrystals of $\mathbf{1}_2 \cdot FeCl_4$ was also measured at room temperature in a similar manner, and the d signal ($g = 2.0887$ and $\Delta H_{pp} = 713$ Oe) (12) again appeared.

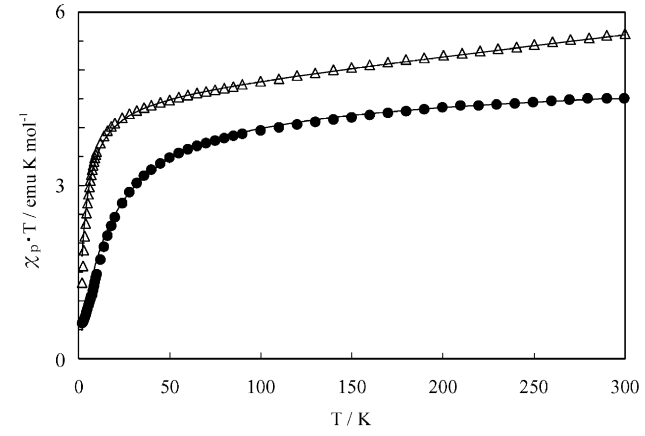

FIG. 5. The temperature dependence of $\chi_p \cdot T$ for the plate crystal of (●)$\mathbf{1}_2 \cdot FeBr_4$ and (△) $\mathbf{1}_2 \cdot FeCl_4$.

However, the π signal could not be detected definitely at room temperature and also at 77 K. Supposedly, the main cause is the spin singlet formation by preferential dimerization of **1** molecules, as seen in the stacking structure of $\mathbf{1}_2 \cdot FeCl_4$.

ACKNOWLEDGMENT

This work was supported by a Grant-in-Aid for Scientific Research on Priority Areas (B) (No. 1224209) from the Ministry of Education, Culture, Sports, Science and Technology, Japan.

REFERENCES

1. P. Day, *Philos. Trans. R. Soc. London Ser. A* **314,** 145 (1985).
2. M. Kurmoo, A. W. Graham, P. Day, S. J. Coles, M. B. Hursthouse, J. L. Caulfied, J. Singleton, F. L. Pratt, W. Hayes, L. Ducasse, and P. Guionneau, *J. Am. Chem. Soc.* **117,** 12209 (1995).
3. L. Martin, S. S. Turner, P. Day, F. E. Mabbs, and E. J. L. McInnes, *Chem. Commun.* 1367 (1997).
4. E. Ojima, H. Fujiwara, K. Kato, H. Kobayashi, H. Tanaka, A. Kobayashi, M. Tokumoto, and P. Cassoux, *J. Am. Chem. Soc.* **121,** 5581 (1999).
5. H. Fujiwara, E. Fujiwara, Y. Nakazawa, B. Z. Narymbetov, K. Kato, H. Kobayashi, A. Kobayashi, M. Tokumoto, and P. Cassoux, *J. Am. Chem. Soc.* **123,** 306 (2001).
6. E. Coronado, J. R. Galán-Mascarós, C. J. Gómez-Garcia, and V. Laukhin, *Nature* **408,** 447 (2000).
7. S. Uji, H. Shinagawa, T. Terashima, T. Yakabe, Y. Terai, M. Tokumoto, A. Kobayashi, H. Tanaka, and H. Kobayashi, *Nature* **410,** 908 (2001).
8. H. Kobayashi, H. Tomita, T. Naito, A. Kobayashi, F. Sakai, T. Watanabe, and P. Cassoux, *J. Am. Chem. Soc.* **118,** 368 (1996).
9. M. Iwamatsu, T. Kominami, K. Ueda, T. Sugimoto, H. Fujita, and T. Adachi, *Chem. Lett.* 329 (1999).
10. M. Iwamatsu, T. Kominami, K. Ueda, T. Sugimoto, T. Tada, K-i. Nishimura, T. Adachi, H. Fujita, F. Guo, S. Yokogawa, H. Yoshino, K. Murata, and M. Shiro, *J. Mater. Chem.* **11,** 385 (2001).
11. M. Iwamatsu, T. Kominami, K. Ueda, T. Sugimoto, T. Adachi, H. Fujita, H. Yoshino, Y. Mizuno, K. Murata, and M. Shiro, *Inorg. Chem.* **39,** 3810 (2000).
12. T. Kominami, T. Matsumoto, K. Ueda, T. Sugimoto, K. Murata, M. Shiro, and H. Fujita, *J. Mater. Chem.* **11,** 2089 (2001).
13. A. Altomare, M. C. Burlea, M. Gamalli, M. Cascarano, C. Giacovazzo, A. Guagliardi, and G. Polidre, *J. Appl. Crystallogr.* **27,** 435 (1994).
14. A. Altomare, M. C. Burlea, M. Gamalli, G. L. Cascarano, C. Giacovazzo, A. Guagliardi, A. G. G. Moliterni, G. Polidre, and R. Spagna, *J. Appl. Crystallogr.* **32,** 115 (1999).
15. P. T. Beurskens, G. Admiraal, G. Beurskens, W. P. Bosman, D. De Gelder, R. Israel, and J. M. M. Smith, *in* "Technical Report of the Crystallography Laboratory," University of Nijmegen, The Netherlands, 1994.
16. TeXsan, "Crystal Structure Analysis Package", Molecular Structure Corporation, Houston, TX, 1985&1992.
17. E. König, "Landolt–Bornstein, Group II: Atomic and Molecular Physics, vol. 2, Magnetic Properties of Coordination and Organometallic Transition Metal Compounds," Springer-Verlag, Berlin, 1966.

18. L. Pauling, *The Nature of the Chemical Bond*, 3rd edn. Cornell University Press, Ithaca, New York, 1960.
19. H. Yamakado, T. Ida, A. Ugawa, K. Yakushi, K. Awaga, Y. Maruyama, K. Imaeda, and H. Inokuchi, *Synth. Met.* **62,** 169 (1994).
20. K. Ueda, M. Goto, M. Iwamatsu, T. Sugimoto, S. Endo, N. Toyota, K. Yamamoto, and H. Fujita, *J. Mater. Chem.* **8,** 2195 (1998).
21. K. Ueda, Y. Kamata, M. Iwamatsu, T. Sugimoto, and H. Fujita, *J. Mater. Chem.* **9,** 2979 (1999).